Published in final edited form as:
Nature. 2011 April 14; 472(7342): 213–216. doi:10.1038/nature09868.

Distinct Representations of Olfactory Information in Different Cortical Centers

Dara L. Sosulski, **Maria V. Lissitsyna**[1], **Tyler Cutforth**[2], **Richard Axel**[*], and **Sandeep Robert Datta**[1]

Department of Neuroscience and the Howard Hughes Medical Institute, College of Physicians and Surgeons, Columbia University, New York, New York 10032, USA

Abstract

Sensory information is transmitted to the brain where it must be processed to translate stimulus features into appropriate behavioral output. In the olfactory system, distributed neural activity in the nose is converted into a segregated map in the olfactory bulb. In this study we ask how this ordered representation is transformed in higher olfactory centers. We have developed a tracing strategy to define the neural circuits that convey information from individual glomeruli in the olfactory bulb to the piriform cortex and the cortical amygdala. The spatial order in the bulb is discarded in piriform cortex; axons from individual glomeruli project diffusely to the piriform without apparent spatial preference. In the cortical amygdala, we observe broad patches of projections that are spatially stereotyped for individual glomeruli. These projections to the amygdala are overlapping and afford the opportunity for spatially localized integration of information from multiple glomeruli. The identification of a distributive pattern of projections to the piriform and stereotyped projections to the amygdala provides an anatomic context for the generation of learned and innate behaviors.

In vision and touch, information central to perception is ordered in space in the external world and this order is maintained from the peripheral sense organs to the cortex. Olfactory information, however, does not exhibit a discernible spatial order in the physical world and this poses the question of how odors are represented in the brain. In mammals, olfactory perception is initiated by the recognition of odorant molecules by a large repertoire of receptors in the olfactory sensory epithelium[1]. Individual olfactory sensory neurons express one of approximately 1,000 receptors[2–4], and each receptor interacts with multiple odorants. Neurons expressing a given receptor, although randomly distributed within zones of the olfactory epithelium, project with precision to two spatially invariant glomeruli in the olfactory bulb[5–7]. Thus, the randomly distributed population of neurons activated by an odorant in the olfactory epithelium is consolidated into a discrete stereotyped map of glomerular activity in the olfactory bulb[8,9].

[*]Correspondence to ra27@columbia.edu.
[1]Present Address: Department of Neurobiology, Harvard Medical School, Boston, MA 02115, USA
[2]Present Address: Department of Molecular, Cell and Developmental Biology, University of California, Santa Cruz, CA 95064, USA

Supplementary Information is linked to the online version of this paper at www.nature.com/nature.

Author Contributions

S.R.D., D.L.S., and R.A conceived of the project, participated in its development and wrote the manuscript. S.R.D. and D.L.S. developed methods and performed all experiments and data analysis. T.C. generated the MOR 1–3 and 174-9-IRES-GFP mice. M.V.L. performed mouse husbandry and immunostaining.

Author Information

The authors declare no competing financial interests.

How is this highly ordered map of spatially invariant glomeruli represented in the cortex? The projection neurons of the olfactory bulb, mitral and tufted cells, extend an apical dendrite into a single glomerulus and send axons to several telencephalic areas, including a significant input to the piriform cortex and cortical amygdala[10–15]. Electrophysiological studies and optical imaging reveal that individual odorants activate subpopulations of neurons distributed across the piriform without spatial preference[16,17]. The piriform therefore discards the spatial segregation of the bulb and returns to a highly dispersed organization in which different odorants activate unique ensembles of cortical neurons. However, the patterns of neural activity do not allow us to discern whether mitral and tufted cell projections from a given glomerulus to cortical neurons are segregated or distributed, and whether they are random or determined. Distinguishing between these possibilities is important for understanding odor perception because a random representation of odor identity could accommodate learned olfactory behaviors, but is unlikely to specify innate behaviors. Rather, innate olfactory behaviors are likely to result from the activation of genetically determined, stereotyped neural circuits. We have therefore developed a strategy to trace the projections from identified glomeruli in the olfactory bulb to higher olfactory cortical centers.

Mitral and tufted cells that innervate a single glomerulus were labeled by electroporation of tetramethylrhodamine (TMR) dextran under the guidance of a two photon microscope. This technique labels mitral and tufted cells that innervate a single glomerulus and is sufficiently robust to allow the identification of axon termini within multiple higher order olfactory centers (Figs. 1a–1c; Fig. 2; Suppl. Figs.1–4). Labeling of glomeruli in the olfactory bulbs of mice that express GFP under the control of specific odorant receptor promoters permits us to examine potential stereotypy of projections from identical glomeruli (MOR 28-IRES-GFP (n = 8), MOR 1–3-IRES-GFP (n= 13), and MOR 174-9-IRES-GFP (n = 10))[18]. Labeling of random unidentified glomeruli was performed in mice expressing synapto-pHluorin (OMP-IRES-spH), a fluorescent marker that allows us to visualize individual glomeruli[9]. This permits us to sample the projection patterns from multiple different glomeruli (Fig. 1c).

Electroporation of a single glomerulus results in the labeling of 6–17 neurons in the mitral cell layer (mean = 9.2 +/− 0.8; Figure 1e; Suppl. Fig. 1c, 2; see Methods). We have demonstrated that all mitral and tufted cells labeled in this manner innervate a single glomerulus by electroporating TMR dextran into one glomerulus and fluorescein (FITC) dextran into a neighboring glomerulus (Fig. 1d). Examination of the mitral and tufted cells following this two-color electroporation reveals either red or green mitral and tufted cells with only a rare cell labeled simultaneously with the two dyes (1/60 cells, n= 4) (Figs. 1e, 1f). This labeling strategy therefore restricts incorporation of tracer to mitral and tufted cells innervating only one glomerulus.

We observe that projections from individual glomeruli extend to all major olfactory cortical regions including the accessory olfactory nucleus, piriform cortex, olfactory tubercle, cortical amygdala and lateral entorhinal cortex (Fig. 2b, Suppl. Fig. 3). Visualization of the extent of axonal projections was facilitated by the development of a flattened hemi-brain preparation that enables high-resolution imaging of all olfactory centers except the anterior olfactory nucleus, which is obscured by the overlying lateral olfactory tract. The glomeruli we have examined project to all the major olfactory cortical regions independent of the spatial location of the glomerulus within the olfactory bulb (n=21 different glomeruli in the flattened preparation; see below). Each of the different higher olfactory centers receives a qualitatively unique pattern of input from the olfactory bulb (Fig. 2b, Suppl. Fig. 3). In the piriform cortex a distributive representation is observed, whereas in the amygdala mitral cell projections are broad but spatially segregated.

Mitral and tufted cell axons extend to the piriform cortex via the lateral olfactory tract (LOT). We observe that axonal branches exit the LOT at right angles and extend upward to densely and diffusely project to the piriform cortex along the entire anteroposterior axis (Figs. 3a–3c), with no apparent spatial preference in any dimension. High resolution multiphoton imaging reveals varicosities likely to be axonal boutons (Suppl. Fig. 4). The spatial distribution of these varicosities is similar in every field imaged and is independent of glomerular origin, suggesting that mitral and tufted cell synapses with piriform neurons are distributed throughout the piriform cortex (Suppl. Fig. 5). The density of these varicosities within the piriform cortex is also similar regardless of the identity of the electroporated glomerulus, further suggesting that each glomerulus makes a similar number of synapses (MOR1–3: 10.2 +/− 0.57 μM of axon per varicosity; M72 (1): 9.9 +/− 0.65 and M72 (2): 10.1 +/− 0.36 μM of axon per varicosity; Suppl. Figs. 4–5). The highly dispersed pattern of projection to the piriform cortex is observed from every glomerulus examined independent of its identity or location within the olfactory bulb (n = 21; Suppl. Fig. 6). On visual inspection, the patterns of projection from two identical glomeruli are no more similar than the patterns of projection observed from two different glomeruli.

We performed hierarchical and k-means clustering to determine whether the observed patterns of projections from different glomeruli are quantitatively distinguishable (see Methods). We were unable to identify any parameters, including axon fiber positions, density of TMR labeling, center of mass X and Y coordinates and centroid X and Y coordinates, that reliably distinguish the projection patterns from different glomeruli (Suppl. Table 1). All measured parameters were similar upon comparison of the projection patterns from identical or different glomeruli (Suppl. Fig. 7).

Cross-correlation analysis was performed to compare the patterns of piriform projections from different glomeruli (see Methods, Suppl. Fig. 8 for detailed explanation of method and interpretation). The correlograms comparing identical and distinct glomeruli display an extended region of moderate correlation (Figs. 3d–3f). These data suggest that the dispersed pattern of projections is largely homogeneous in density over several spatial scales (Suppl. Fig. 9) and indicate that the patterns are similar for each of the 24 glomeruli we have examined. The similarity of correlograms from identical and different glomeruli provide further evidence that the pattern of piriform projections does not differ for each of the distinct glomerulus types. Thus, the mitral cells innervating an individual glomerulus discard the insular and invariant spatial segregation of the bulb and project dense, dispersed axons to the piriform cortex with no discernible spatial bias.

We next examined the patterns of projections of single glomeruli to the cortical amygdala. The cortical amygdala consists of three nuclei: the anterior cortical, posterolateral cortical, and posteromedial cortical nuclei. The posteromedial cortical nucleus, a major site of innervation from the accessory olfactory bulb[19], receives no discernible input from any of the glomeruli of the main olfactory bulb we have examined (Figs. 4a–4c, n = 33 glomeruli in the en face preparation, see Methods), and we observe relatively sparse projections anterior to the posterolateral nucleus. We therefore restrict our analysis to the posterolateral cortical nucleus. The patterns of projection from individual glomeruli in the posterolateral nucleus reveal dense, patchy axonal projections that exhibit a focal nexus surrounded by a less dense halo of fibers (Figs. 4a–4f). Despite the diffuse nature of projections, different glomeruli appear to send fibers to anatomically distinct and spatially invariant regions of the posterolateral cortical amygdala (Figs. 4a–4f). For example, projections from the MOR 1–3 glomerulus consistently occupy the most medial aspect of the posterolateral nucleus, whereas projections from the MOR28 glomerulus terminate more laterally. These conclusions are evident on visual inspection and are supported by more quantitative analysis.

K-means clustering using relevant parameters extracted from the amygdala projection patterns after image alignment (center of mass X coordinate, X position of medial-most fiber, absolute medial fiber density, ratio of lateral/medial fiber density) was performed on the projections from three identified glomeruli, MOR 1–3 (n=5), MOR 174-9 (n =5), and MOR 28 (n=4). This cluster analysis correctly assigns glomerular identity for 79% of the samples examined (one-way MANOVA, $p = 0.0006$, $\alpha = 0.05$).

We have performed normalized cross-correlation analysis to further compare the projection patterns from different glomeruli. Cross-correlation analysis reveals a single peak in the correlogram that reflects the more focal nature of projections to this brain region than in the piriform (Figs. 4h–4g). The correlograms between the projection patterns of identical glomeruli reveal peaks that exhibit a small displacement from the center (Figs 4h, 4i; Suppl. Figs. 10–11a–c, 12g–h, Suppl. Tables 2 and 3). Cross-correlation using images of projection patterns from different glomeruli exhibit more varied and often very large displacements (Fig. 4j; Suppl. Figs. 10–11d–j and 12i, Suppl. Tables 2 and 3). These data indicate that the cortical amygdala receives spatially stereotyped projections from individual glomeruli. Although individual glomeruli project to fixed positions, extensive overlap is observed for the projections from different glomeruli. The apparently random pattern of projections in the piriform and the determined pattern in the amygdala are likely to provide the anatomic substrates for distinct olfactory-driven behaviors mediated by these two brain regions.

Insight into the logic of olfactory perception will depend upon an understanding of the how the highly ordered glomerular map is represented in higher olfactory centers. Previous experiments have employed the injection of tracer molecules into the bulb or cortex, to relate the spatial position of projection neurons in the bulb with their targets in higher olfactory centers[10–15]. These experiments predate the ability to identify specific glomeruli,[6] precluding a determination as to whether projections from a single mitral/tufted cell or a single glomerulus are random or stereotyped.

We have defined a neural circuit that conveys olfactory information from specific glomeruli in the olfactory bulb to the piriform cortex and the cortical amygdala. A distributive representation of neurons in the sensory epithelium is converted into a topographic map in the bulb upon the convergence of like axons onto spatially invariant glomeruli[5,6]. The piriform discards this spatial order; axons from individual glomeruli project diffusely to the piriform without apparent spatial preference. Neurons from every glomerulus elaborate similar axonal arbors and quantitative analyses fail to identify features that may distinguish the individual projection patterns. This data is in accord with retrograde tracings using rabies virus that reveal the convergence of multiple, spatially distributed glomeruli on a small number of piriform neurons (Miyamichi et al., this issue). A distributive representation of glomerular projections in piriform is also observed upon anterograde tracing of individual mitral cells following Sindbis virus infection (Ghosh et al., submitted).

Optical imaging and electrophysiological studies of neural responses to odors reflect these anatomic transformations. Distributed neural activity in the sensory epithelium of the nose is transformed in the bulb, with each odor eliciting distinct spatial patterns of glomerular activity[8,9]. A second transformation is apparent in the piriform cortex where individual odorants activate unique ensembles of neurons that are distributed without discernible spatial order[16,17]. These neurons also exhibit discontinuous receptive fields; neurons within an ensemble responsive to a given odor respond to multiple, structurally dissimilar odors[16,20]. The dispersed projections to the piriform provide an anatomic substrate for the generation of these patterns of neural activity.

One model consistent with both the anatomy and physiology invokes the random convergence of excitatory inputs from mitral cells onto piriform neurons such that each piriform neuron would sample a random combination of glomerular inputs. If the connections from bulb to cortex are indeed random, then the representation of the quality of an odorant or its valence in the piriform must be imposed by experience. Odorants, however, can elicit innate behavioral responses, suggesting that a second area of the brain must receive determined inputs from the olfactory bulb. The pattern of projections to the posterolateral amygdala implicate this structure in the generation of innate olfactory-driven behaviors. This suggestion is in accord with the finding that disruption of the amygdala abrogates innate, odor-driven behaviors but leaves learned olfactory responses intact[21,22].

The olfactory circuits we describe in the mouse are reminiscent of the architecture of the olfactory system in *Drosophila*[23] despite the six hundred million years of evolution that separate the two organisms. In *Drosophila*, neurons expressing a given odorant receptor are distributed throughout the antenna and converge on spatially invariant glomeruli in the antennal lobe. Information from the antennal lobe bifurcates with one branch exhibiting spatially invariant projections to the lateral horn, a brain region mediating innate olfactory behaviors. A second branch projects to the mushroom body, a structure required for learned olfactory responses. This anatomic and functional bifurcation provides a context in which to consider the generation of the various forms of olfactory-driven behavior in both flies and mice. Our data suggest that innate olfactory behaviors derive from determined neural circuits selected over evolutionary time, whereas learned behaviors may be mediated by the selection and reinforcement of random ensembles of neurons over the life of an organism.

Methods Summary

Single glomeruli and their associated mitral and tufted cells were labeled in adult mice via electroporation of 3kD tetramethylrhodamine dextran (Invitrogen) under a twophoton microscope (Prairie Technologies). Glass electrodes were backfilled with dye and guided to a glomerulus center, and current was applied to the back of the pipette (50V, 30msec pulses, 2Hz, 7–10 minutes, repeated 2–4 times, Grass Technologies). Afterwards, animals were allowed to recover for 5 days before sacrifice. Excised brains were prepared for imaging either by flattening the cortex of the right hemisphere or surgical excision of the cortical amygdala. TMR dextran signal was amplified by antibody staining (Jackson Immunoresearch), and samples were counterstained (NeuroTrace 435, Invitrogen). Images were acquired using multiphoton excitation on a Zeiss 710 or a Prairie In Vivo microscope. Image Z-stacks of the piriform cortex or cortical amygdala were aligned using SPM8 and Photoshop, and then quantified using ImageJ and custom-written Matlab code (Mathworks, Inc). Detailed descriptions of methods are available as supplementary methods.

Supplementary Material

Refer to Web version on PubMed Central for supplementary material.

Acknowledgments

We thank members of the Axel and Datta labs for comments and advice, Ben Shykind for labeled OR mice, Sean X. Luo for image alignment advice, Daniel M. Bear for cross-correlation analysis advice, Dirk Padfield for Matlab code, Rachel Wilson for comments on the manuscript, and Phyllis Kisloff for manuscript preparation assistance. Financial support was provided by a Helen Hay Whitney Foundation Fellowship, a Career Award in the Medical Sciences grant from the Burroughs Wellcome Fund and funding from the National Institutes of Health through the NIH Director's New Innovator program (DP2-OD-007109) (S. R. D.), a Ruth L. Kirschstein National Research Service Award (NRSA) predoctoral fellowship from the NIH (D.L.S.), the Howard Hughes Medical Institute, and a grant from the Foundation for the National Institutes of Health through the Grand Challenges in Global Health initiative (R.A.).

References

1. Buck L, Axel R. A novel multigene family may encode odorant receptors: a molecular basis for odor recognition. Cell. 1991; 65:175–187. [PubMed: 1840504]
2. Malnic B, Hirono J, Sato T, Buck LB. Combinatorial receptor codes for odors. Cell. 1999; 96:713–723. [PubMed: 10089886]
3. Chess A, Simon I, Cedar H, Axel R. Allelic inactivation regulates olfactory receptor gene expression. Cell. 1994; 78:823–834. [PubMed: 8087849]
4. Niimura Y, Nei M. Evolutionary changes of the number of olfactory receptor genes in the human and mouse lineages. Gene. 2005; 346:23–28. [PubMed: 15716099]
5. Ressler KJ, Sullivan SL, Buck LB. Information coding in the olfactory system: evidence for a stereotyped and highly organized epitope map in the olfactory bulb. Cell. 1994; 79:1245–1255. [PubMed: 7528109]
6. Mombaerts P, et al. Visualizing an olfactory sensory map. Cell. 1996; 87:675–686. [PubMed: 8929536]
7. Vassar R, et al. Topographic organization of sensory projections to the olfactory bulb. Cell. 1994; 79:981–991. [PubMed: 8001145]
8. Rubin BD, Katz LC. Optical imaging of odorant representations in the mammalian olfactory bulb. Neuron. 1999; 23:499–511. [PubMed: 10433262]
9. Bozza T, McGann JP, Mombaerts P, Wachowiak M. In vivo imaging of neuronal activity by targeted expression of a genetically encoded probe in the mouse. Neuron. 2004; 42:9–21. [PubMed: 15066261]
10. Haberly LB, Price JL. The axonal projection patterns of the mitral and tufted cells of the olfactory bulb in the rat. Brain Res. 1977; 129:152–157. [PubMed: 68803]
11. Scott JW, McBride RL, Schneider SP. The organization of projections from the olfactory bulb to the piriform cortex and olfactory tubercle in the rat. J Comp Neurol. 1980; 194:519–534. [PubMed: 7451680]
12. Price JL. An autoradiographic study of complementary laminar patterns of termination of afferent fibers to the olfactory cortex. J Comp Neurol. 1973; 150:87–108. [PubMed: 4722147]
13. Luskin MB, Price JL. The distribution of axon collaterals from the olfactory bulb and the nucleus of the horizontal limb of the diagonal band to the olfactory cortex, demonstrated by double retrograde labeling techniques. J Comp Neurol. 1982; 209:249–263. [PubMed: 7130455]
14. Buonviso N, Revial MF, Jourdan F. The Projections of Mitral Cells from Small Local Regions of the Olfactory Bulb: An Anterograde Tracing Study Using PHA-L (Phaseolus vulgaris Leucoagglutinin). Eur J Neurosci. 1991; 3:493–500. [PubMed: 12106481]
15. Ojima H, Mori K, Kishi K. The trajectory of mitral cell axons in the rabbit olfactory cortex revealed by intracellular HRP injection. J Comp Neurol. 1984; 230:77–87. [PubMed: 6096415]
16. Stettler DD, Axel R. Representations of odor in the piriform cortex. Neuron. 2009; 63:854–864. [PubMed: 19778513]
17. Rennaker RL, Chen CF, Ruyle AM, Sloan AM, Wilson DA. Spatial and temporal distribution of odorant-evoked activity in the piriform cortex. J Neurosci. 2007; 27:1534–1542. [PubMed: 17301162]
18. Shykind BM, et al. Gene switching and the stability of odorant receptor gene choice. Cell. 2004; 117:801–815. [PubMed: 15186780]
19. de Olmos J, Hardy H, Heimer L. The afferent connections of the main and the accessory olfactory bulb formations in the rat: an experimental HRP-study. J Comp Neurol. 1978; 181:213–244. [PubMed: 690266]
20. Poo C, Isaacson JS. Odor representations in olfactory cortex:"sparse" coding, global inhibition, and oscillations. Neuron. 2009; 62:850–861. [PubMed: 19555653]
21. Blanchard DC, Blanchard RJ. Innate and conditioned reactions to threat in rats with amygdaloid lesions. J Comp Physiol Psychol. 1972; 81:281–290. [PubMed: 5084445]
22. Slotnick BM. Olfactory discrimination in rats with anterior amygdala lesions. Behav Neurosci. 1985; 99:956–963. [PubMed: 3843312]

23. Vosshall LB, Stocker RF. Molecular architecture of smell and taste in Drosophila. Annu Rev Neurosci. 2007; 30:505–533. [PubMed: 17506643]

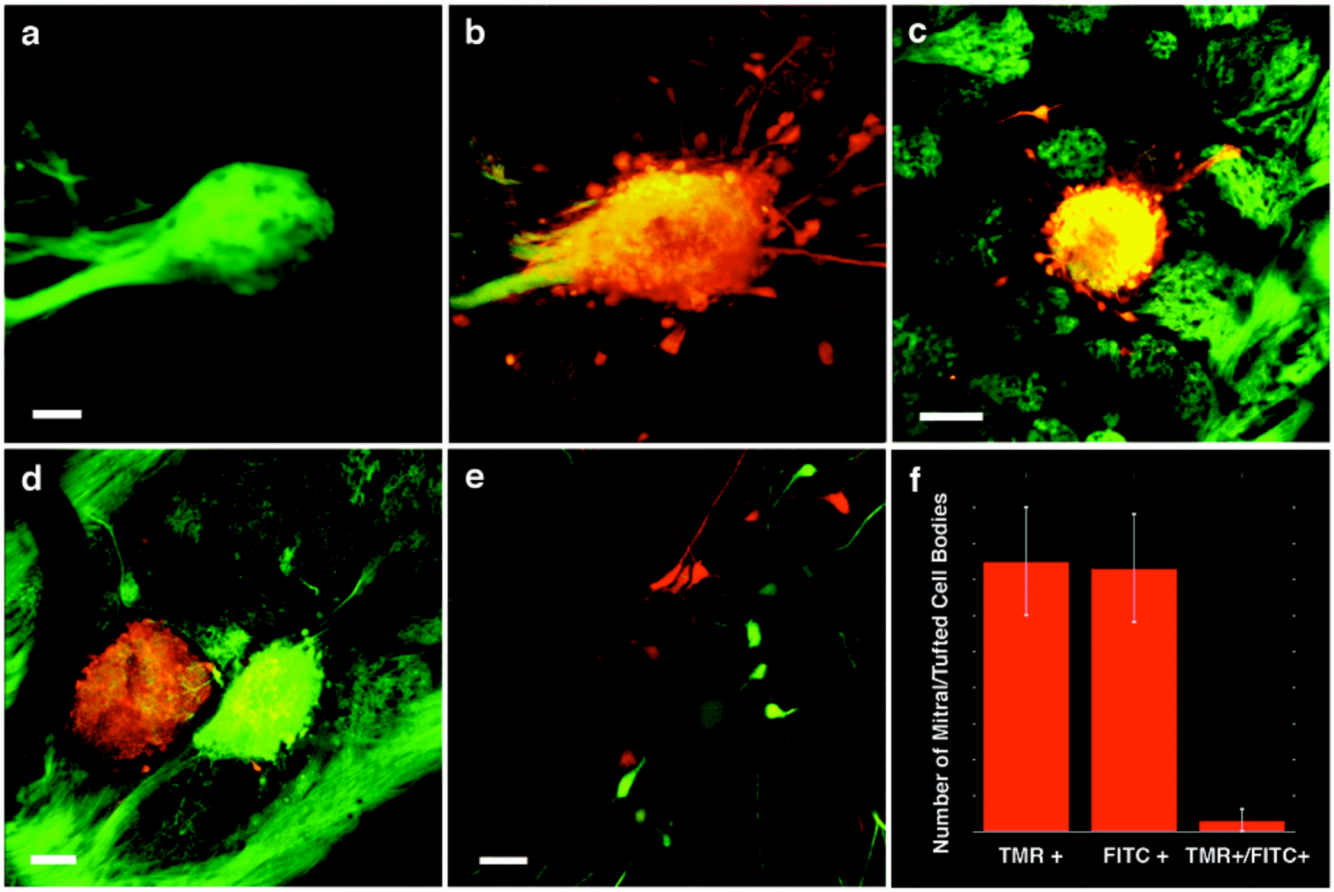

Figure 1. Targeted electroporation of tetramethylrhodamine (TMR) dextran labels cells that innervate a single glomerulus in the olfactory bulb

A mouse olfactory bulb in which MOR 174-9 is labeled with GFP, before **(a)** and after **(b)** electroporation with TMR dextran (scale bar = 40 μM). **(c)** Image similar to **(a)** where electroporation was performed in a mouse in which synaptopHluorin is expressed in all glomeruli (OMP-IRES-spH, green); note that labeling (red) is confined to a single glomerulus (scale bar = 85 μM). **(d)** Control experiment in an OMP-IRES-spH mouse in which neighboring glomeruli were electroporated with TMR dextran (red, left) and fluorescein dextran (green, right, scale bar = 45 μM). **(e)** Labeling of mitral cells (red, green) as a result of the experiment in **(d)**. **(f)** Quantification of the overlap in mitral cell labeling in experiments similar to **(d)** (n = 4).

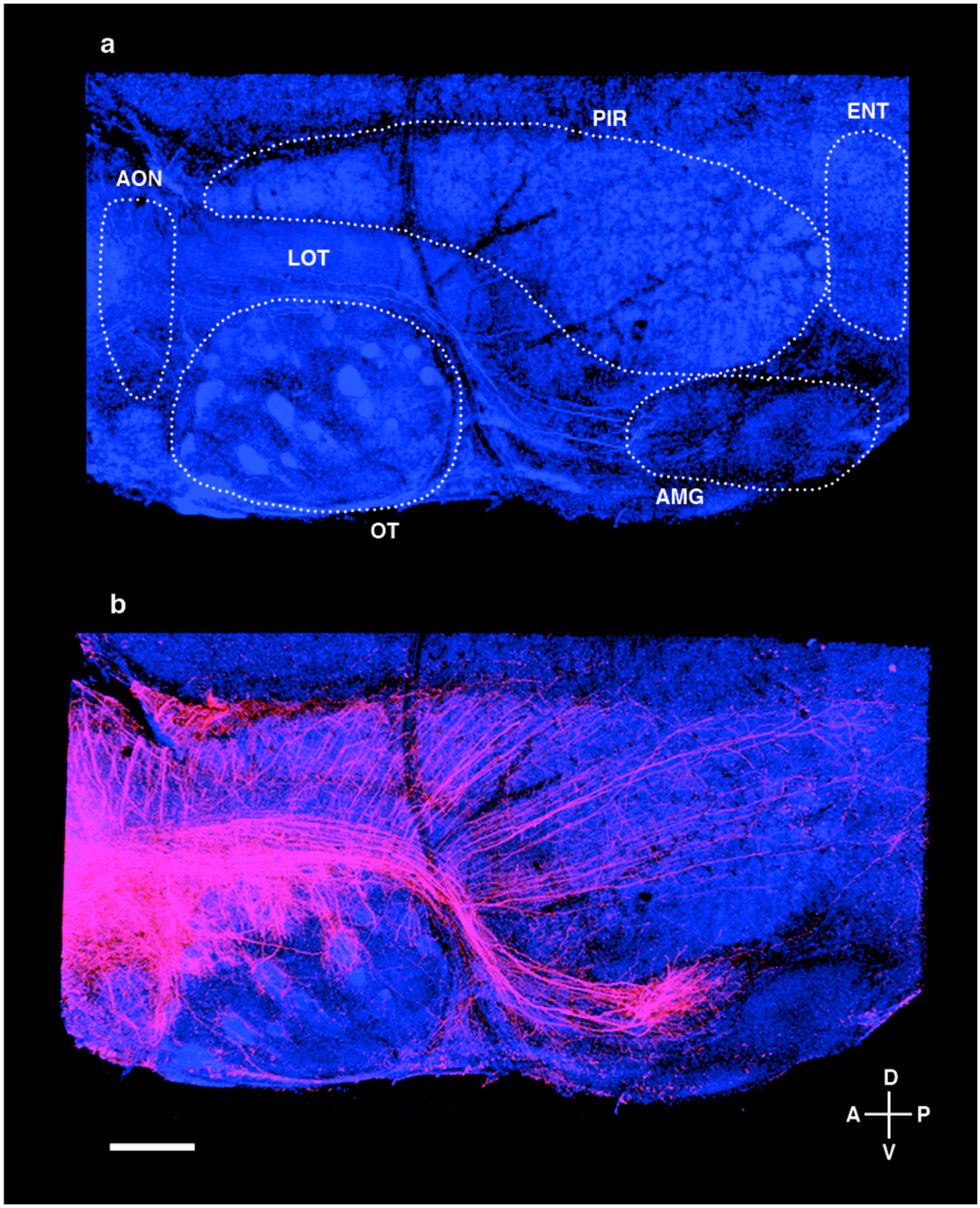

Figure 2. Mitral/tufted cells connected to a single glomerulus exhibit distinct patterns of projections to several areas of the olfactory cortex

(a) A flattened hemi-brain preparation of the olfactory cortex with nuclei identified by counterstain (blue, NeuroTrace 435) and relevant structures outlined in white (LOT = lateral olfactory tract; AON = anterior olfactory nucleus; OT = olfactory tubercle; PIR = piriform cortex; AMG = cortical amygdala; ENT = lateral entorhinal cortex). **(b)** A hemi-brain from a mouse in which a single glomerulus was electroporated with TMR-dextran (red). Note the unique pattern of projection in each of the olfactory areas (scale bar = 700 μM, see also Suppl. Fig. 3).

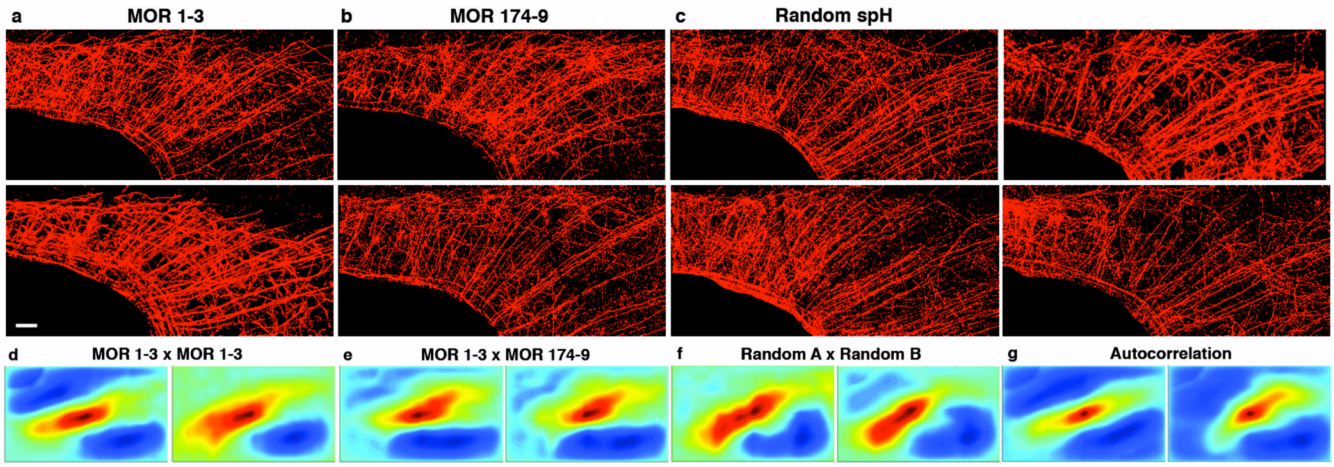

Figure 3. Projections from single glomeruli to piriform cortex are disperse, homogeneous and indistinguishable

Images of axons innervating the piriform cortex (red) from mitral and tufted cells that connect to the glomerulus corresponding to MOR 1–3 (scale bar = 500 μM) **(a)**, MOR 174-9 **(b)** or a random selection of glomeruli labeled with TMR-dextran **(c)**. Correlograms plotted using the matrix of correlation coefficients generated by normalized cross-correlation of two MOR 1–3 piriforms **(d)**, a MOR 1–3 and a MOR 174-9 piriform **(e)**, and two piriforms in which random glomeruli were labeled **(f)**. Cross-correlation is performed using aligned images of projection patterns as seen in **(a)–(c)**. **(g)** Autocorrelograms generated using methods from **(d)** in which a labeled piriform is compared to itself. Note that correlograms in **(g)** are essentially indistinguishable from the correlograms in **(d)–(f)**.

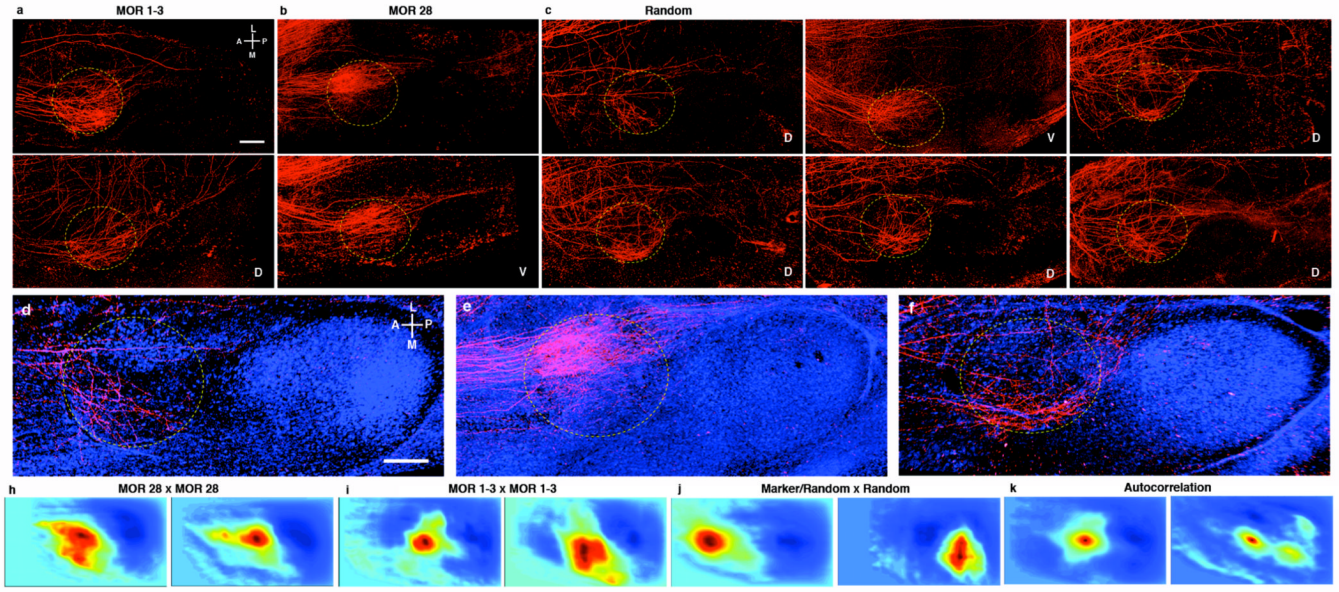

Figure 4. Projections from single glomeruli to the cortical amygdala are broad, patchy and stereotyped

Images of the cortical amygdala reveal similar projections from the mitral and tufted cells that connect to the MOR 1–3 glomerulus in two different brains (circle = approximate posterolateral cortical nucleus boundary; scale bar = 400 μM) **(a)**, but projections that are distinct from those of mitral/tufted cells connected to the MOR 28 glomerulus **(b)** or six randomly selected glomeruli **(c)**. "D" or "V" in the bottom right corner of the image indicates whether the electroporated glomerulus was located dorsally or ventrally in the bulb. **(d)–(f)** Counterstained images from a subregion of images in **(a)–(c)** displaying a closer view of projection patterns (scale bar = 400 μM). Correlograms plotted using the matrix of correlation coefficients generated by normalized cross-correlation of MOR 28 × MOR 28 projection patterns within the cortical amygdala **(h)**, MOR 1–3 × MOR 1–3 projection patterns **(i)**, or projection patterns from glomeruli of different types **(j)**. **(k)** Autocorrelograms of the PLCo from two labeled glomeruli correlated with themselves. Note that in the en bloc preparation shown here, the lateral/medial axis (indicated by the orientation bars) is synonymous with the dorsal/ventral axis, as this region of brain is curved.